

# A RESPONSE-MATRIX METHOD FOR THE CALCULATION OF NEUTRON PULSE HEIGHT DISTRIBUTIONS IN MCNP

**S. Prasad\*, S. D. Clarke, S. A. Pozzi, E.W.Larsen**

Department of Nuclear Engineering and Radiological Sciences, University of Michigan,  
Ann Arbor, MI 48109  
\*shikhap@umich.edu

## ABSTRACT

We apply the Response-Matrix Method for the calculation of neutron pulse height distribution (Response-Matrix PHD) in order to compute PHD efficiently by reducing computation time and minimizing variance. The PHD calculations and their associated uncertainty are compared for polyethylene-shielded and lead-shielded setups with a  $^{252}\text{Cf}$  source. These comparisons are made for three cases: laboratory measured PHD, Response-Matrix PHD Source Biased, and fully analog MCNPX-PoliMi PHD. It is found that the Response-Matrix PHD greatly improves the figure of merit when compared to the fully analog case. The Response-Matrix PHD Source Biased method utilizes the source biasing method which is the most applicable given the source energy spectrum of the  $^{252}\text{Cf}$ . Finally, different simulations of source-shield configuration are compared with their laboratory measured results and show very good agreement thereby validating the computationally robust Response Matrix method.

*Keywords:* pulse height distribution, variance reduction, liquid scintillators, MCNPX-PoliMi, nonproliferation, measurement

## 1. INTRODUCTION

Detection of shielded special nuclear material (SNM) is significant in nuclear nonproliferation. The neutron energy spectrum is a signature that is useful in identifying and characterizing SNM which may be obtained using liquid scintillation detectors. Simulations are needed in order to design an effective scintillation-based measurement system; these are most commonly performed using the Monte Carlo method. Pulse height distributions (PHD) neutron detector response for liquid scintillators unveil information about the neutron energy spectrum and are thus useful in identifying and characterizing sources. However, the widely used MCNP code does not have the ability to calculate scintillator neutron detector responses.

In the past, these distributions have been computed using specialized algorithms to process MCNP output [1, 2]. The method proposed here utilizes a single detector response matrix which operates on the incident neutron energy to calculate the detector pulse height distribution. This method is general, and can be applied to any source-shielding configuration; one only needs to tally the neutron energy spectrum incident on the detector face. Any standard MCNP variance reduction techniques may be applied to calculate the incident neutron energy distribution. In the

paper Response-Matrix PHD method is applied with variance reduction techniques to shielded neutron sources and compared to analog MCNPX-PoliMi data.

## 2. NUMERICAL METHOD

The Response-Matrix PHD method makes use of an MCNPX-PoliMi calculated response matrix to calculate the pulse height distribution. It is also required to know the neutron energy spectrum incident on the detector. This energy spectrum may be calculated using any standard variance reduction technique applicable to the problem. The formulation of the method is described below:

### 2.1 MCNPX-PoliMi Response Matrix

The response matrix used in the calculation of Response-Matrix PHD contains information about the EJ-309 liquid scintillator's intrinsic efficiency. The rows of the matrix correspond to energies ranging from 0.2 MeV to 15 MeV with increments of 20 keV (741 energy bins) while the columns correspond to light output ranging from 0.01 MeVee to 10.07 MeVee with increments of 10 keVee (1007 light output bins). The sum of all light outputs (or columns) for a given energy (row) gives the total intrinsic detection efficiency at that energy. Thus, more generally for  $m$  energy rows and  $n$  light output columns the response matrix is:

$$R = \begin{bmatrix} R_{E1,L1} & \cdots & R_{E1,Ln} \\ \vdots & \ddots & \vdots \\ R_{Em,L1} & \cdots & R_{Em,Ln} \end{bmatrix}$$

The response matrix is created using analog MCNPX-PoliMi simulations to calculate the energy deposited which were converted to light using appropriate coefficients; here a separate MCNPX-PoliMi case was run for each energy bin in the matrix. The neutrons simulated are monodirectional.

### 2.2 Pulse Height Distribution Formulation

Since a response-matrix element represents the intrinsic efficiency for an incident energy  $E$  and light output  $L$ , its product with the number of incident neutrons at a given energy  $E$  yields the total number of neutrons detected for  $E$  at light output  $L$ . Thus, if these products are summed over all incident energies as in Eq. (1), one obtains the total number of counts for the light output bin  $L$ . Similarly counts can be obtained for all light output bins yielding a complete pulse height spectrum. The formula governing this method using MCNP is given as following:

$$N(L) = \sum_{i=1}^m \hat{n} \cdot J^+(E_i) \cdot A \cdot R(E_i, L) \cdot \Delta E_i \quad (1)$$

$N(L)$  = total counts for a given light output  $L$        $A$  = area of the detector  
 $L$  = a given light output bin       $R(E_i, L)$  = response matrix element at  $E_i$   
 $E_i$  =  $i^{\text{th}}$  energy bin      and  $L$   
 $\hat{n}$  = vector normal to the detector face       $\Delta E_i$  = energy bin width about  $E_i$   
 $J^+$  = partial current towards detector face

The F1 tally in MCNP counts the number of particles crossing a user specified surface. Thus, the number of particles entering the detector face is calculated by the F1 tally and has the following relationship [4]:

$$F1_{MCNP}(E_i) = \hat{n} \cdot J^+ \cdot A \cdot \Delta E_i \quad (2)$$

Substituting Eq. (2) in Eq. (1) we obtain the simple relationship for counts in a light output bin:

$$N(L) = \sum_{i=1}^m F1_{MCNP}(E_i) \cdot R(E_i, L) \quad (3)$$

The Response-Matrix PHD method utilizes Eq. (3) to calculate the pulse height distribution. The assumption here is that there is no overlap of neutrons in a pulse. The MCNP F1 tally used in this result can be calculated using MCNP5, MCNPX or MCNPX-PoliMi. The F1 tally does not need to be run in analog mode and can therefore make use of applicable variance reduction techniques.

### 2.3 Radial Leakage Correction Factor

As mentioned in section 2.1 the response matrix has been constructed for neutrons that travel monodirectionally and perpendicular to the detector face. However, the neutrons coming out from the shielded  $^{252}\text{Cf}$  isotropic source are not monodirectional and perpendicular to the detector face. These neutrons have a greater chance of leaking out of the lateral sides of the detector and in general will have a shorter pathlength or a smaller likelihood to scatter in the scintillator detector, and thus get detected. As a result the PHD calculated with the Response-Matrix PHD method will be an overestimate since the response matrix underestimates lateral leakage through the sides. For larger distances (more than half a meter source detector distance in the given setup) this effect will be minimal since the angle subtended between the source and the edge of the detector will be small and thus the particle direction will be closer to a perpendicular monodirectional beam. However, as the source gets closer to the detector the spread of a particle's incident direction with respect to the detector face increases and thus this effect becomes more dominant as shown below in Fig. 1(a) for a 10 cm source detector distance with 5.08 cm (2 inches) of polyethylene shield.

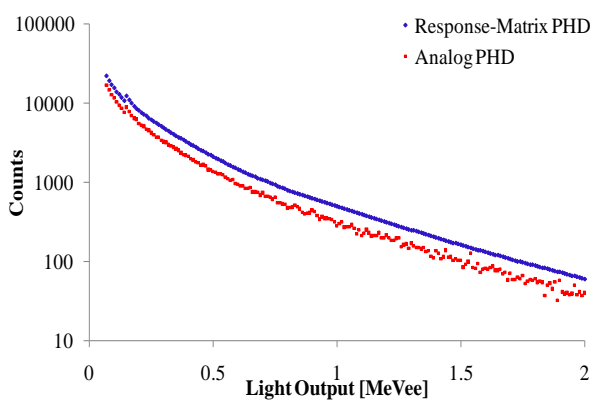


**Figure 1(a): Response-Matrix PHD without radial leakage correction compared to analog.**

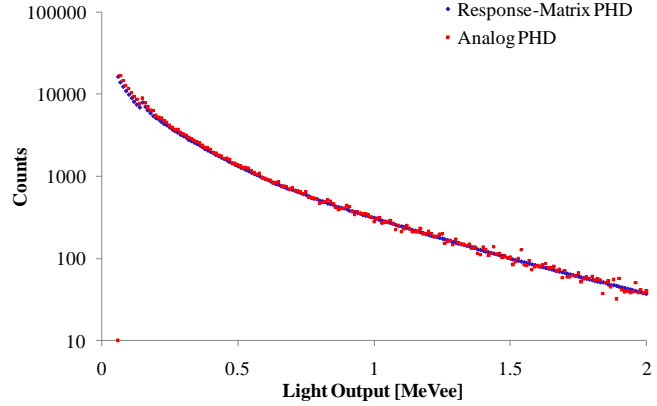


**Figure 1(b) Response Matrix PHD with radial leakage correction compared to analog.**

As seen in Fig. 1(a) the discrepancy is significant between the Response Matrix PHD which uses the response matrix constructed using monodirectional neutrons and the MCNPX-PoliMi PHD which correctly models the incident angle of the neutron and the subsequent interactions. In order to correct for this discrepancy caused due to incident angle of the neutrons we formulate a radial leakage correction factor:

$$\zeta = \Phi_{unmodified} / \Phi_{beam} \quad (4).$$

Since we obtain higher counts using the Response Matrix PHD due to larger intrinsic efficiencies, the correction factor should correctly account for greater leakage from the detector sides to reduce the intrinsic efficiencies. In order to accomplish this task we need to calculate the factor by which the rate of the pathlength creation differs in the case where the particles are not incident in a perpendicular beam. A ratio  $\zeta$ , of the volumetric flux (rate of pathlength creation in a given volume [4]) for the given setup with unmodified particle direction,  $\Phi_{unmodified}$ , to the case where the particles in setup are made monodirectionally incident on the detector face,  $\Phi_{beam}$  is calculated. This ratio given in Eq. (4) is calculated for each energy group. Each light output's intrinsic efficiency in an energy group is multiplied by its corresponding  $\zeta$  to yield the correct intrinsic efficiency as:

$$\varepsilon_{corrected}(E_m, L_n) = \varepsilon_{beam}(E_m, L_n) \zeta(E_m) \quad (5).$$

As seen in Fig 1(b) after incorporating the radial leakage correction factors the agreement between the Response Matrix PHD and analog MCNPX PoliMi PHD is excellent.

## 2.4 Variance Reduction Techniques

Analog Monte Carlo simulations can be long and time consuming. In order to increase the usefulness of Monte Carlo, variance reduction techniques are used to reduce the uncertainty and complete simulations in shorter run-times. There are various variance reduction options available in MCNP such as source biasing, geometry splitting, point detectors, DXTRAN, to name a few. It is important to choose the options that efficiently reduce uncertainty, while minimizing simulation run-times [4].

A typical fission spectrum has fewer neutrons towards higher energies, thus an F1 tally will tend to have greater uncertainty in these regions. Nonetheless, higher energies are important since bigger light pulses are caused due to higher energies deposited. Therefore, it is important to reduce uncertainty of the F1 tally towards higher energies. Hence, for the method we have applied the source biasing technique to obtain a uniform variance distribution.

In the source biasing method the user specifies the desired probability distribution,  $\hat{p}$  or the biases. Based on these biases new weights,  $\hat{w}$  are calculated such that the product of original weight  $w_0$  and probability  $p_0$  are preserved:

$$w_0 \cdot p_0 = \hat{w} \cdot \hat{p} \quad (6)$$

In order to obtain a uniform distribution throughout the spectrum instead of low variance in certain regions and higher in the others, a flat distribution is input as the desired probability density distribution, the new weights are then calculated according to Eq. (6). Thus, given that  $w_0$  is unity, it can be gleaned that  $\hat{w}$  must follow the spectral shape of  $p_0$  (if  $\hat{p}$  is a flat distribution) such that the product  $\hat{w} \cdot \hat{p}$  is preserved as shown in Eq (6). This relationship is demonstrated using MCNP results as discussed in the Section 4.

## 3. LABORATORY MEASUREMENTS

Measurements were performed to validate simulation results as shown in Fig. 2. A strong  $^{252}\text{Cf}$  source emitting nearly  $3.3 \times 10^5$  neutrons per second placed 30 cm from detector was shielded with different thicknesses of polyethylene and lead shields. The measurements were performed at the Detection for Nuclear Nonproliferation Group Laboratory (DNNG), University of Michigan. A  $^{137}\text{Cs}$  source was used for calibration. A 12-bit digitizer was used. The threshold for detection was determined to be 70 keVee.

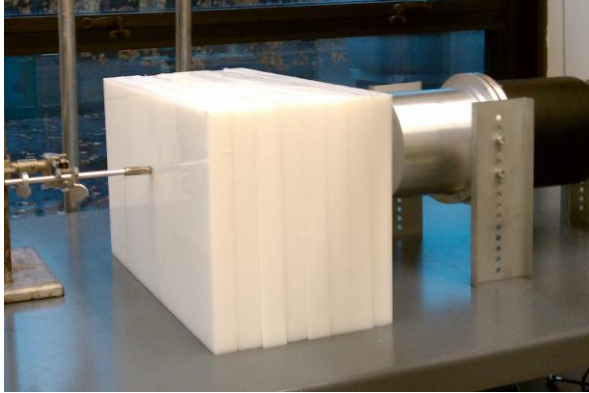


**Figure 2(a): Measurement setup with  $^{252}\text{Cf}$  source (left), 20.3 cm of polyethylene (middle) and EJ-309 detector (right).**

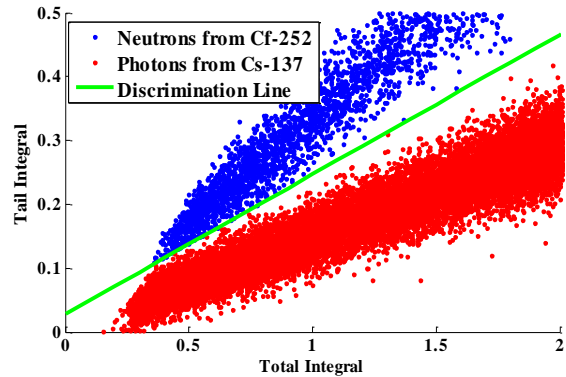


**Figure 2(b): Pulse shape discrimination between neutrons (blue) and gammas (red) for the setup with no shielding.**

Pulses signal the detection of particles. Acquisition window is 100 points long where each point is 4 ns wide. The pulses were discriminated between neutrons and gammas based on their tail to total integrals as shown in Fig. 2(b). Neutrons interact with the nuclei in the scintillator and thus result in larger tails compared to gamma-rays which interact with electrons. Therefore, in Fig. 2(b) points corresponding to higher tail integral values for the same total integral value of the pulse are from neutrons and are those points found above the discrimination line.

#### 4. MONTE CARLO SIMULATIONS

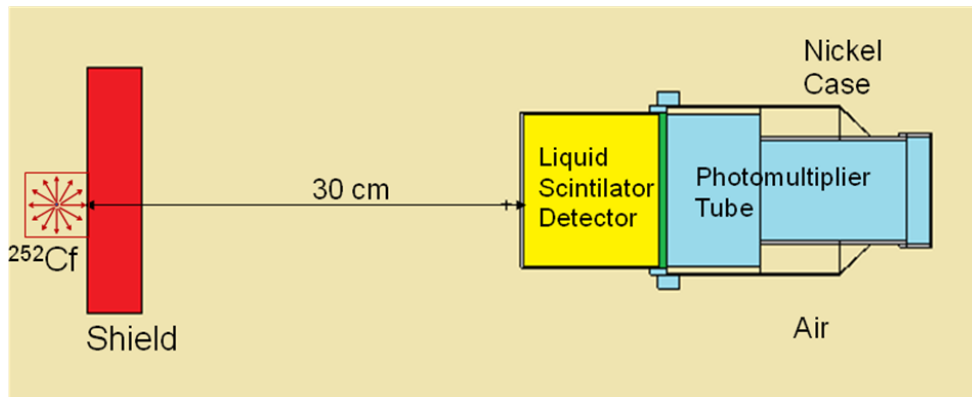


**Figure 3: Shielded  $^{252}\text{Cf}$  setup with an EJ-309 liquid scintillator**

The measurement setup shown in Fig. 3 contains an isotropic  $^{252}\text{Cf}$  source placed 30 cm from the face of an EJ-309 liquid scintillation detector. In addition to the features modeled in Fig.3 the iron table on which the detector rests and the concrete floor are also modeled. The source is shielded by lead or polyethylene rectangular blocks that are 5.08 cm, 10.16 cm, 15.24 cm and 20.32 cm thick. The detector is a cylinder with a radius of 6.34 cm and a length of 12.51 cm. Its chemical

composition is 54.8% hydrogen and 45.2% natural carbon by number of atoms. The  $^{252}\text{Cf}$  source is modeled only to emit fission spectrum simulated by the Watt spectrum.

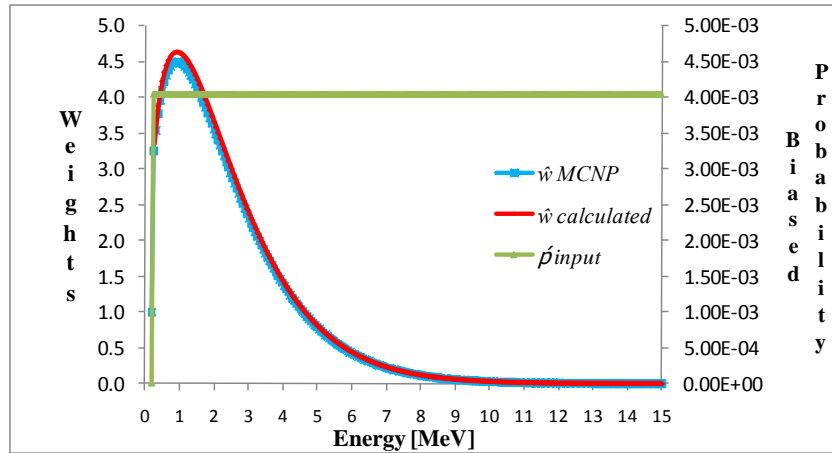


**Figure 4: Source biased new weights, calculated new weights and biased new probability**

As discussed in the previous section describing variance reduction techniques, source biasing requires the user to input a desired distribution of source particles,  $\hat{p}$  (shown in Fig. 4). This desired distribution in our case is a uniform distribution of source particles throughout the spectrum such that a uniform uncertainty distribution is obtained in the F1 tally throughout the energy spectrum. Based on these biased probabilities new weights,  $\hat{w}$  are calculated such that the product of original weight  $w_0$  and probability  $p_0$  are preserved as given by Eq. (6). In Fig. 4 both the MCNP new weights  $\hat{w}$  and those calculated independently using Eq. (6) are in good agreement. Since  $\hat{p}$  is a flat distribution it is expected that the spectral shape of  $\hat{w}$  will be that of a Watt spectrum (as seen in Fig. 4) in order to preserve the original probability distribution  $p_0$  of the Watt spectrum.

## 5. RESULTS & ANALYSIS

This section is divided in four subsections. The first subsection presents the source-biased F1 tally results that give the neutron energy spectrum entering the detector. This incoming neutron energy spectrum is combined with response matrix to yield pulse height distributions. The next two subsections discuss the Response Matrix method results and their statistical uncertainties respectively. Finally, in the last subsection comparisons of the simulation results with the measurement data are shown.

### 5.1 Incident Current on Detector Face using Source Biasing

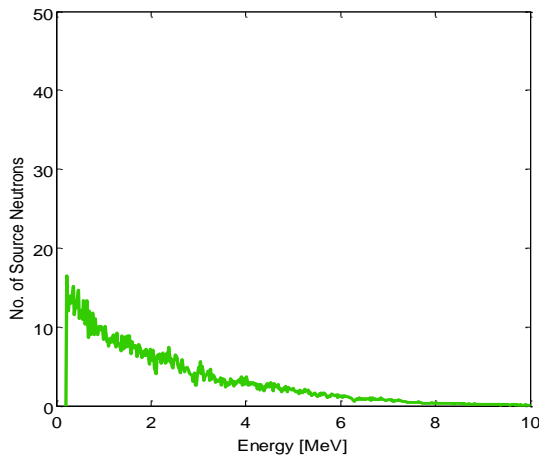


Figure 5(a):  $^{252}\text{Cf}$  neutron spectrum from polyethylene

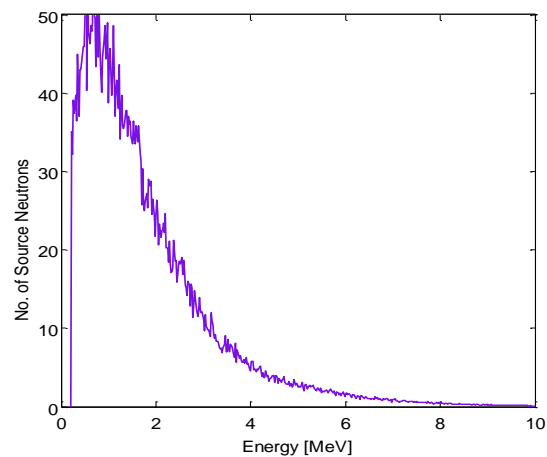


Figure 5(b):  $^{252}\text{Cf}$  neutron spectrum from lead

The F1 tally in MCNP was used to tally the neutron spectrum entering the detector face after leaving the 10.16 cm (4 in) thick polyethylene or lead shields as shown in Fig. 5(a) and 5(b). These cases were run for  $10^7$  source particles but have been normalized to the source strength in the laboratory measurements. As seen above, the spectrum from the polyethylene shield has been heavily moderated and has lost its original Watt spectrum shape. Whereas the spectrum from the lead shield has still retained most of the Watt spectrum shape. Polyethylene is a highly hydrogenous material and is thus very effective in moderating neutrons. Lead is made up of heavy nuclei and is thus not as effective in moderating neutrons. However, lead has several resonances in its elastic scatter cross-sections contributing to the fluctuations seen in the peak of the spectrum in Fig. 5(b) [5].

The MCNP cases were performed with and without variance reduction techniques. The MCNP simulation with variance reduction utilized source biasing as discussed in the previous section to produce uniform uncertainty throughout the energy spectrum as shown in Fig. 6. It can be gleaned that the uncertainty in both cases is relatively flat throughout the energy spectrum. The high uncertainty even for a large number of source particles is expected since each energy bin is only 20



keV in width. Furthermore, in the case of lead shield the spectrum of neutrons has smaller uncertainties for smaller energies and then flattens out. For the purpose of this paper, however, we are interested in the pulse height distribution resulting from a combination of particles in all energy bins and their responses from the MCNPX-PoliMi calculated response matrix as discussed next.

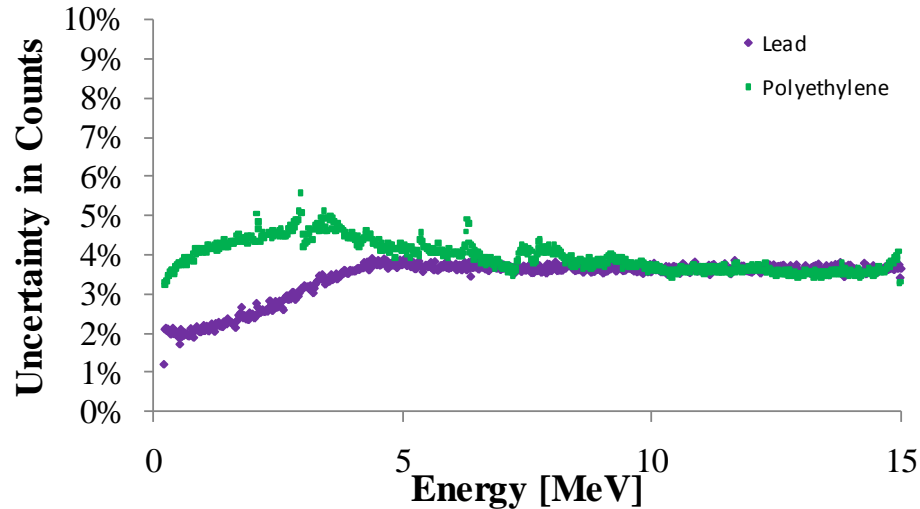


**Figure 6: Percent uncertainty in source biased neutron energy spectrum entering detector**

### 5.2 Pulse Height Distribution Comparison

The F1 tallies or the current of neutrons entering the detector is combined with the response matrix as shown by Eq. 3 to yield pulse height distributions as shown in Fig. 7(a) and 7(b) for 10.16 cm (4 in) thick polyethylene and lead shield respectively. It can be gleaned from these figures that the analog pulse height distribution obtained from MCNPX-PoliMi case and its postprocessor has extremely large variances. However, in the case of Response-Matrix PHD and Response-Matrix PHD Source Biased the pulse height distributions are well converged. The figures are shown only up to 2 MeV since for higher energies the analog pulse height spectrum has almost 100% uncertainty, moreover, the scintillator measurement data can be measured only up to 2 MeV. For this light output range both the Response-Matrix PHD methods, with and without source biasing have very small uncertainty and are therefore difficult to differentiate. The differences between these methods are better illustrated by Fig. 8(a) and 8(b). It can also be observed in Figure 7(a) and 7(b) that the lead pulse height spectrum has higher counts than the polyethylene pulse height spectrum, this behavior is expected given the two energy spectra shown in Figures 5(a) and 5(b): the lead-shielded spectrum is less moderated than the polyethylene-shielded spectrum.

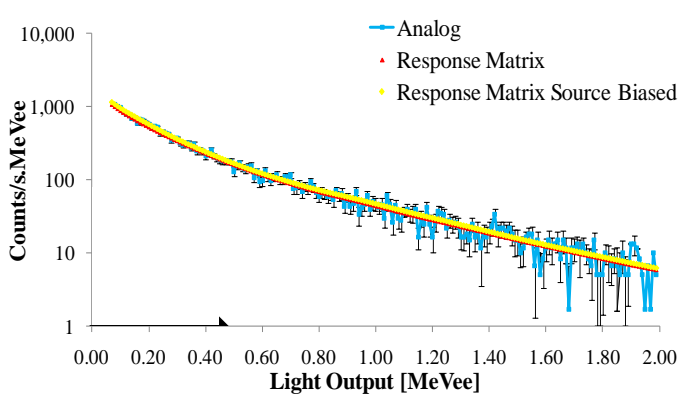


Figure 7(a):  $^{252}\text{Cf}$  PHD from a polyethylene shield

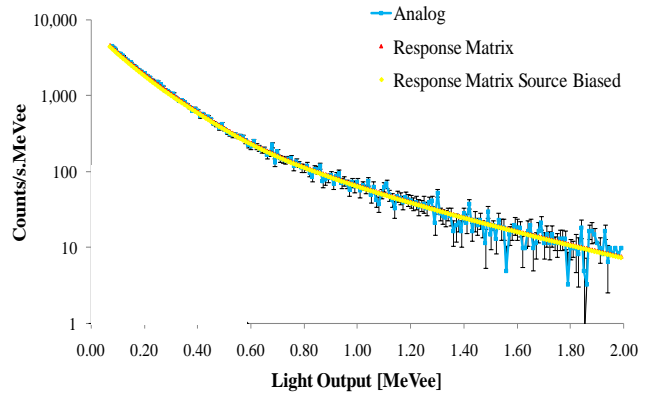


Figure 7(b):  $^{252}\text{Cf}$  PHD from a lead shield

### 5.3 Pulse Height Distribution Uncertainty Comparison

This section discusses the statistical uncertainty in the calculation of the pulse height distributions. The uncertainty in the pulse height distribution for 10.16 cm (4 in) thick polyethylene or lead shields with  $10^7$  source particles obtained by using the three methods: analog PHD, Response-Matrix PHD and Response-Matrix PHD Source Biased is shown in Fig. 8(a) and 8(b). The advantage of using the Response-Matrix PHD is evident from these graphs. The analog PHD results in uncertainty over 10% just about 500 keVee and reaches nearly a 100% about 2 MeVee. The Response-Matrix PHD method is a significant improvement over the analog case where the uncertainty ranges between 1% and 2% both cases, however, it shows a gradually increasing trend which crosses 10% around 5 MeVee. The Response-Matrix PHD Source Biased, however, provides the best improvement. For this method the uncertainty remains constant at about 1%, nearly three orders of magnitude improvement for light output greater than 1 MeVee for the same number of source particles and slightly reduced runtime in MCNP.

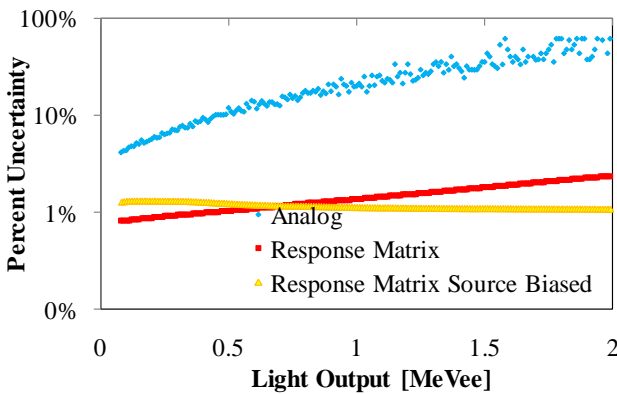


Figure 8(a): Uncertainty in  $^{252}\text{Cf}$  PHD from polyethylene

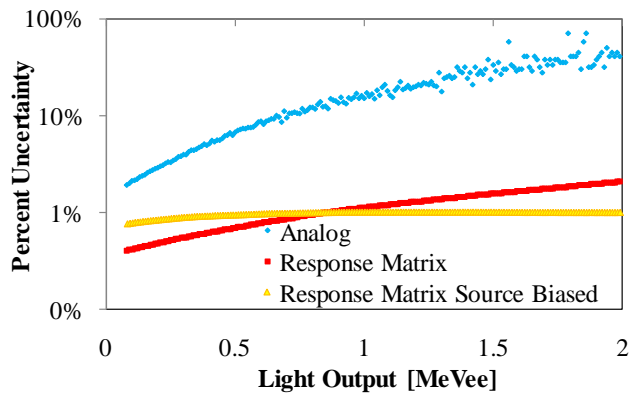


Figure 8(b): Uncertainty in  $^{252}\text{Cf}$  PHD from lead

**Table I: Figure of Merit Improvement with Response Matrix over the Entire Pulse Height Distribution**

Shielding Material	5.08 cm (2 in)	10.16 cm (4 in)	15.24 cm (6 in)	20.32 cm (8 in)
Polyethylene	6.5	8.2	8.3	8.0
Lead	3.2	3.6	3.9	4.2

FOM is calculated using the standard MCNP convention:

$$\text{FOM} \equiv 1/(\text{R}^2\text{T}) \quad (7)$$

Where, R is the sample relative standard deviation of the mean, and T is the computational time [4]. In Table I factors of improvement in the figure of merit (FOM) for the entire pulse height distribution range or over all light output bins are shown. If one had to calculate FOM factors for individual low light output bins they would be close to the values listed above but as we move towards higher light output bins the FOM improvement factors increase by orders of magnitude. The FOM improvement factors listed in Table I are mainly representative of FOM improvement factors of the many low light output bins because the number of counts in the high light output bins are very few.

The FOM improvement factor is calculated as a ratio between the FOM for the Response Matrix PHD method (no additional variance reduction used) to the analog PHD. The FOM improvement is significant for polyethylene and lead shields, however, it is substantially greater in the case of polyethylene shields where it is over a factor of 8 for all thicknesses (except the 5.08 cm where it is 6.5). For the lead shields it varies between a factor of 3 and 4. FOM improvement factors for individual light output bins in the higher end of the spectrum can be greater than three orders of magnitude evident from Fig. 8(a) and 8(b), however, in Table 1 when we discuss the FOM improvement over the entire PHD spectrum.

Thus, the greatest advantage is attained by the using the Response-Matrix PHD Source Biased method. The Response-Matrix PHD and the Response-Matrix PHD Source Biased method are also different from the analog PHD method because they do not need to post-process an additional data bank with the information about all collisions and the energy deposited. The detector response is already contained in the MCNPX-PoliMi calculated response matrix. Furthermore, since the response matrix has fixed dimensions ( $m$  by  $n$ ) the number of floating point operations performed to process the data (Eq. 3) is independent of the number of source particles, it is always  $2mn-n$ . Given 741 energy bins and 1007 light bins for cases discussed here, there are merely 1.5 million floating point operations performed for any number of source particles using the Response Matrix PHD method. However, in the analog case the post processor will do more work and run for longer times for a greater number of source particles since there will be more collisions to follow. Additionally,

the analog case will also consume greater storage space to save the data bank as the number of source particles is increased.

### 5.4 Comparison of Response Matrix PHD with Measured Data

The computational advantage of the Response Matrix method with and without standard MCNP variance reduction techniques has been verified above by comparing the results with analog MCNPX-PoliMi cases. However, the true value of the technique is proven by comparing the results with measured data. The measurement technique has been discussed in Section 3, here we discuss the results.

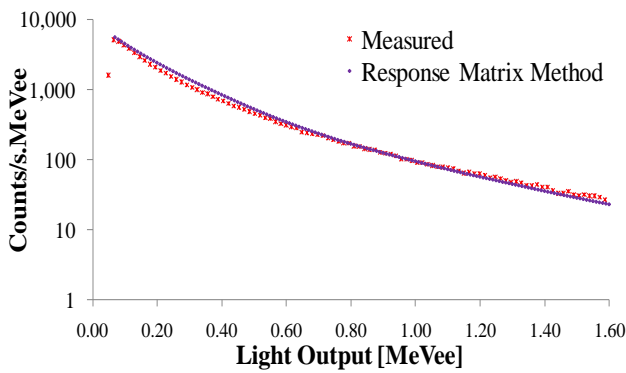


Figure 9(a): Lead shield 5.08 cm (2 in)

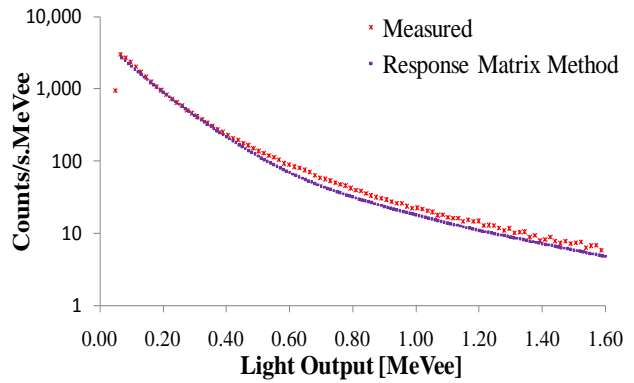


Figure 9(b): Lead shield 20.32 cm (8 in)

As seen in Fig. 9(a) and 9(b) the simulated Response Matrix method results of lead shielded  $^{252}\text{Cf}$  source agree very well with the measured data. This agreement is even better for the case with 5 cm of lead. For 20 cm of lead the simulated Response Matrix counts are slightly lower than the measurement beyond 0.40 MeVee.

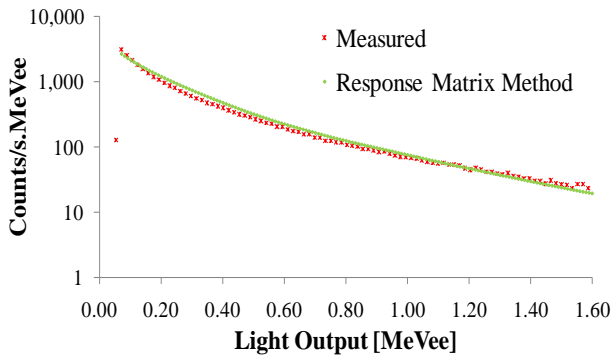


Figure 10(a): Polyethylene shield 5.08 cm (2 in)

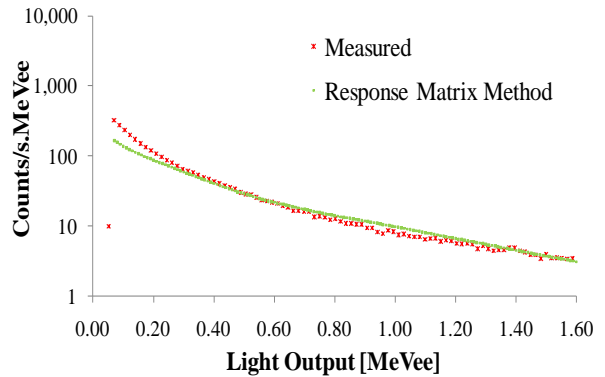


Figure 10(b): Polyethylene shield 20.32 cm (8 in)

In Fig. 10(a) and 10(b) measurements with polyethylene shields have been shown. The agreement in case of 5 cm of polyethylene is good but a little higher than the measurement. The agreement in case of 20 cm of polyethylene is generally good but can be improved to better simulate the measured spectrum. For the 20 cm case the simulated counts are lower below 0.3 MeV. The disagreement in this low region is very likely due to the misclassification of neutrons in the PSD process as shown in Fig 2(b). For low light outputs gammas and neutrons can overlap in the PSD plot, this overlap becomes more important when the shield becomes increasingly moderating and gives lower energy neutrons that yield smaller light pulses. A more general reason for the discrepancy between the measured and the simulated could be the empirically found light conversion coefficients that convert the energy deposited in the detector into the light output. Work continues to refine these coefficients to achieve excellent agreement in various measurement configurations.

## 6. CONCLUSION

Pulse height distributions are important for characterizing sources. They describe the energy deposition behavior of particles. Monte Carlo codes such as MCNP5 cannot calculate neutron pulse height distribution for scintillators [4]. MCNPX-PoliMi and its associated post-processor can calculate pulse height distributions, however, calculations can be done only in analog mode resulting in time consuming runs and post processing. The method proposed here, Response-Matrix PHD utilizes a single detector response matrix which operates on the incident neutron energy to calculate the detector pulse height distribution. The Response-Matrix PHD is also applied with source biasing as it is not required to be run in the analog mode. The simulation setup comprises of the  $^{252}\text{Cf}$  source placed 30 cm away from the EJ-309 liquid scintillator detector with a 10.15 cm (4 in) thick polyethylene or lead shield in front of the source.

A comparison of the three methods is made for  $10^7$  neutron source particles. It is evident that the Response-Matrix PHD method greatly reduces variance throughout the pulse height spectrum. In general, a FOM improvement by a factor of 8 is achieved in the case of polyethylene shields and a factor of 3-4 times is achieved in the case of lead shields over the entire PHD. These factors can be as much as a few orders of magnitude for individual high light output bins. Furthermore, using the Response-Matrix PHD Source Biased not only decreases the variance even more but keeps it constant throughout the spectrum. The statistical uncertainty in the source biased case is usually constant about 1%, whereas in the analog case the uncertainty reaches nearly a 100% only at about 2 MeV. Furthermore, the analog case requires storage of large data files, and requires time consuming post-processing of these files. Comparisons with DNNG laboratory measured data for 5.08 cm and 20.32 cm polyethylene and lead shields are also very promising and show excellent agreement in general. Work continues to refine the light conversion coefficients that can further improve the agreement between measured and simulated results. Future work on this method will

include examining other variance reduction techniques such as DXTRAN and point detector tallies in addition to investigating more demanding shielding configurations.

## 7. REFERENCES

- [1] S. A. Pozzi, E. Padovani, M. Marseguerra. MCNP-PoliMi: A Monte Carlo Code for Correlation Measurements, Nucl. Instr. Meth. A, 513, pp. 550 – 558, 2003.
- [2] S. Pozzi, E. Padovani, M. Flaska, and S. Clarke. *MCNP-PoliMi Post-Processing Code Ver. 1.9*. Oak Ridge National Laboratory Internal Report, ORNL/TM-2007/33, 2007.
- [3] S. A. Pozzi, S. D. Clarke, M. Flaska, and P. Peerani. Pulse Height Distributions of Neutrons and Gamma-Rays from Plutonium Oxide. Nucl. Instr. Meth. A 608, pp. 310 – 315, 2009.
- [4] *MCNP5 User's Manual, Volume 1*. Los Alamos National Laboratory, LA-UR-03-1987, April 2003.
- [5] Evaluated Nuclear Data Files, ENDF VII, <http://www.nndc.bnl.gov/sigma/>